

A NUCLEON-NUCLEUS ELASTIC SCATTERING MODEL FOR LAHETTM

R. E. Prael
Mail Stop B226
Los Alamos National Laboratory
Los Alamos, NM 87545
(505)667-7283

D. G. Madland
Mail Stop B243
Los Alamos National Laboratory
Los Alamos, NM 87545
(505)667-6007

Published in: *Proceedings of the 1996 ANS Topical Meeting Radiation Protection and Shielding, No. Falmouth, Massachusetts, April 21-25, 1996*, p. 251 (1996).

ABSTRACT

A model for elastic scattering of protons and neutrons has been adapted for the LAHET Monte Carlo code. New optical-model cross sections are included, as well as a new algorithm for sampling the scattering distribution.

I. INTRODUCTION

The LAHET¹ Monte Carlo code for the transport and interaction of nucleons, pions, muons, light ions, and antinucleons has been upgraded by the addition of an elastic scattering model for neutrons above 15 MeV and protons above 50 MeV. Earlier elastic scattering in LAHET had been limited to neutrons below 100 MeV using the Bechetti-Greenlees potential. In our new approach, the Monte Carlo methodology has been adapted from the HERMES² code. However, the sampling algorithm for the center-of-mass scattering angle has been completely rewritten. More significantly, the elastic cross section data has been replaced below 400 MeV by using a global medium-energy nucleon-nucleus phenomenological optical-model potential. This approach is an intermediate step in the effort to provide a library of both elastic and non-elastic cross sections from a global optical-model potential for LAHET usage.

II. NUCLEON ELASTIC SCATTERING CROSS SECTIONS FROM 50 MEV TO 400 MEV

The tabulated elastic scattering cross sections were generated with an interim³ global medium energy nucleon-nucleus phenomenological optical-model potential. The potential is based upon a relativistic Schrödinger representation and is applicable to neutron and proton incident energies in the range 50 – 400 MeV and a target mass range of $20 \leq A \leq 220$. Nuclear deformation effects have been ignored in this implementation.

The starting point for this work was the spherical proton optical potential of Schwandt *et al.*⁴ for the range 80 – 180 MeV. This potential was modified to optimally reproduce experimental proton total reaction cross sections as a function of energy while allowing only minimal deterioration in the fits to other elastic proton scattering observables. Further modifications in the energy dependence of the absorptive potential were found necessary to extrapolate the modified potential to energies above

180 MeV. At this point explicit isospin was introduced and the potential was converted to a neutron-nucleus potential by use of standard Lane model assumptions and by accounting approximately for the Coulomb correction. Final comparisons of predicted and measured observables for both protons and neutrons (proton reaction cross sections, neutron total cross sections, and elastic differential cross sections) were made for ^{27}Al , ^{56}Fe , and ^{208}Pb . The results were generally good.

The neutron and proton elastic cross sections so generated are tabulated in LAHET for 9 mass values (^{12}C , ^{16}O , ^{27}Al , ^{40}Ca , ^{56}Fe , ^{81}Br , ^{107}Ag , ^{138}Ba , and ^{208}Pb) and 20 energies (50, 60, 70, 80, 90, 100, 110, 120, 140, 160, 180, 200, 225, 250, 275, 300, 325, 350, 375, and 400 MeV) between 50 MeV and 400 MeV. Above 400 MeV, the tabulations from HERMES are used. Above 50 MeV, the HERMES tabulation for ^4He is used. Below 50 MeV the HERMES neutron elastic cross section tabulation is used and has been extended with additional optical model calculations to lower and higher masses to minimize mass extrapolation error; in this energy range, the cross sections are tabulated for 27 masses. Proton elastic scattering vanishes below 50 MeV in this implementation. A selection of the cross sections are shown in figure 2.

III. SAMPLING ALGORITHM FOR THE ANGULAR DISTRIBUTION

The current model² for the sampling distribution of the COM scattering angle is given by

$$\frac{d\sigma}{d\Omega} \sim \left(\frac{J_1(x)}{x} \right)^2$$

$$x = 2R \sin(\theta/2) / \bar{\lambda}$$

$$R = (1.4 fm) A^{1/3} + \bar{\lambda}$$

$$\cos \theta = 1 - \bar{\lambda}^2 x^2 / 2R^2$$

which provides a probability distribution for x^2 or $\cos \theta$. The implementation is by a table of 98 equally-probable (1%) intervals in the variable x^2 , with an approximate asymptotic distribution for the last 2% of the distribution. In practice, the sampling range is always restricted by

$$x \leq 2R\bar{\lambda}$$

equivalent to the limit $\cos \theta \geq -1$.

In figure 2, a test calculation for $p(\cos \theta)$ vs. θ is shown for the center-of-mass angular distribution for 84 MeV neutrons scattered by ^{27}Al . The plot shown is an actual tabulation from sampling the distribution using 10^8 random samples of the algorithm. The location of the first few zeros of the Bessel function in the distribution is apparent. At larger angles, the histogram-like structure is indicative of the 1% bin structure of the tabulated distribution, and the minima at larger angles have been obscured by the bin structure of the tables.

As originally developed², sampling from the distribution was truncated near the first minimum of the mathematical distribution above, and no scattering was allowed into larger angles. However, a recent paper by Nakashima *et al.*⁵ concludes that this original formulation underestimates the

off-axial neutron flux observed in their shielding benchmark experiments on the transmission of neutrons through iron shields. Since up to 14% of the scattering will take place to angles beyond the first minimum, the new model may improve the comparison with these experiments.

Our long term objective is to provide a general sampling scheme which can represent directly the angular distributions obtained from optical model calculations. However, the simple model as implemented is amenable to possible improvements. One such method would be to constrain the sampling to match the calculated first moment of the scattering distribution. Another option would be to force the first minimum in the sampling distribution to match the first minimum of the calculated distribution.

IV. EXAMPLE CALCULATIONS

The presence of an elastic scattering channel in LAHET for protons (and neutrons above 100 MeV) adds entirely new calculational features. Most notably, damage calculations are modified by the effect of recoiling nuclei from proton elastic scattering above 50 MeV and from the improved neutron treatment at all energies. In our first example, figure 3, the damage energy spectrum is shown for 100 MeV protons on a 0.1 cm thick aluminum slab. The damage component from elastic scattering is a significant fraction of the total and would not have appeared in earlier LAHET calculations; in this example, the elastic contribution is 30% of the mean total recoil energy deposited and 41% percent of the mean total damage energy. The minima of the sampling distribution are apparent in the results; there is a significant contribution from the large-angle scatters above the first minimum.

A second example of 100 MeV neutrons incident on 0.5 cm thick aluminum is shown in figure 4. The old treatment for neutron elastic scattering could adequately represent only the *mean* recoil energy deposition, and only below 100 MeV. The new method models the probability distribution of recoil energies in a more realistic manner and, as seen in figure 3, leads to an increase in the damage component; the change in the elastic treatment results in a 29% increase in the mean total recoil energy but a 69% increase in the mean total damage energy. Again, the structure in the calculation is evident; the earlier LAHET result contains only a contribution from the large-angle scattering.

The presence of a proton elastic scattering channel provides another mechanism for energy deposition through recoil of the target nuclei. The magnitude of the effect can be seen in figure 5, where the effects of proton elastic scattering are contrasted to multiple scattering of protons. A longitudinal energy deposition calculation (MeV/cm) is shown for 256 MeV protons on ^{27}Al . The elastic scattering deposits energy at higher energies and lowers the energy deposition peak without shifting it greatly. The two mechanisms produce effects, however, of comparable magnitude. Continuing the proton elastic scattering below 50 MeV might change the results by a small amount.

V. CONCLUSIONS

The elastic scattering model discussed above employs cross sections generated from a physically based optical-model potential appropriate to the energy range in which they are applied in LAHET

and broadens considerably the mass range for the tabulated cross sections at low energies. The LAHET implementation is an interim step in the long-range objective of determining elastic and nonelastic reaction rates through cross sections obtained by a global nucleon-nucleus optical potential for the energy range 20 MeV to 2 GeV. This is an important goal because such a potential provides simultaneous flux conservation among the elastic, all nonelastic, and total cross sections for both protons and neutrons.

The strongest motivation for implementing the interim model discussed above is to improve the damage calculation capability; the effects shown are quite dramatic. However, the overall simulation quality is also improved by the new elastic scattering treatment. The impact on energy deposition and primary beam dispersion and degradation is relatively smaller, but still significant in the context of benchmark calculations as described in the paper by Nakashima⁵.

REFERENCES

1. Richard E. Prael and Henry Lichtenstein, "User Guide to LCS: The LAHET Code System", LA-UR-89-3014, Los Alamos National Laboratory (September 1989).
2. P. Cloth *et al.*, *HERMES - A Monte Carlo Program System for Beam-Materials Interaction Studies*, Kernforschungsanlage Jülich GmbH, Jül-2203 (May 1988).
3. D. G. Madland, *Proceedings of a Specialist's Meeting on Preequilibrium Reactions, Semmering, Austria, February 10-12, 1988*, Edited by B. Strohmaier (OECD, Paris, 1988), p. 103-116.
4. P. Schwandt *et al.*, *Phys. Rev. C* **26**, 55 (1982).
5. Hiroshi Nakashima *et al.*, "Transmission Through Shields of Quasi-Monoenergetic Neutrons Generated by 43- and 68-MeV Protons: Part II Iron Shielding Experiment and Analysis for Investigating Computational Method and Cross Section Data", submitted to *Nuclear Science and Engineering* (Nov. 1995).

LAHETTM is a trademark of the Regents of the University of California and the Los Alamos National Laboratory.

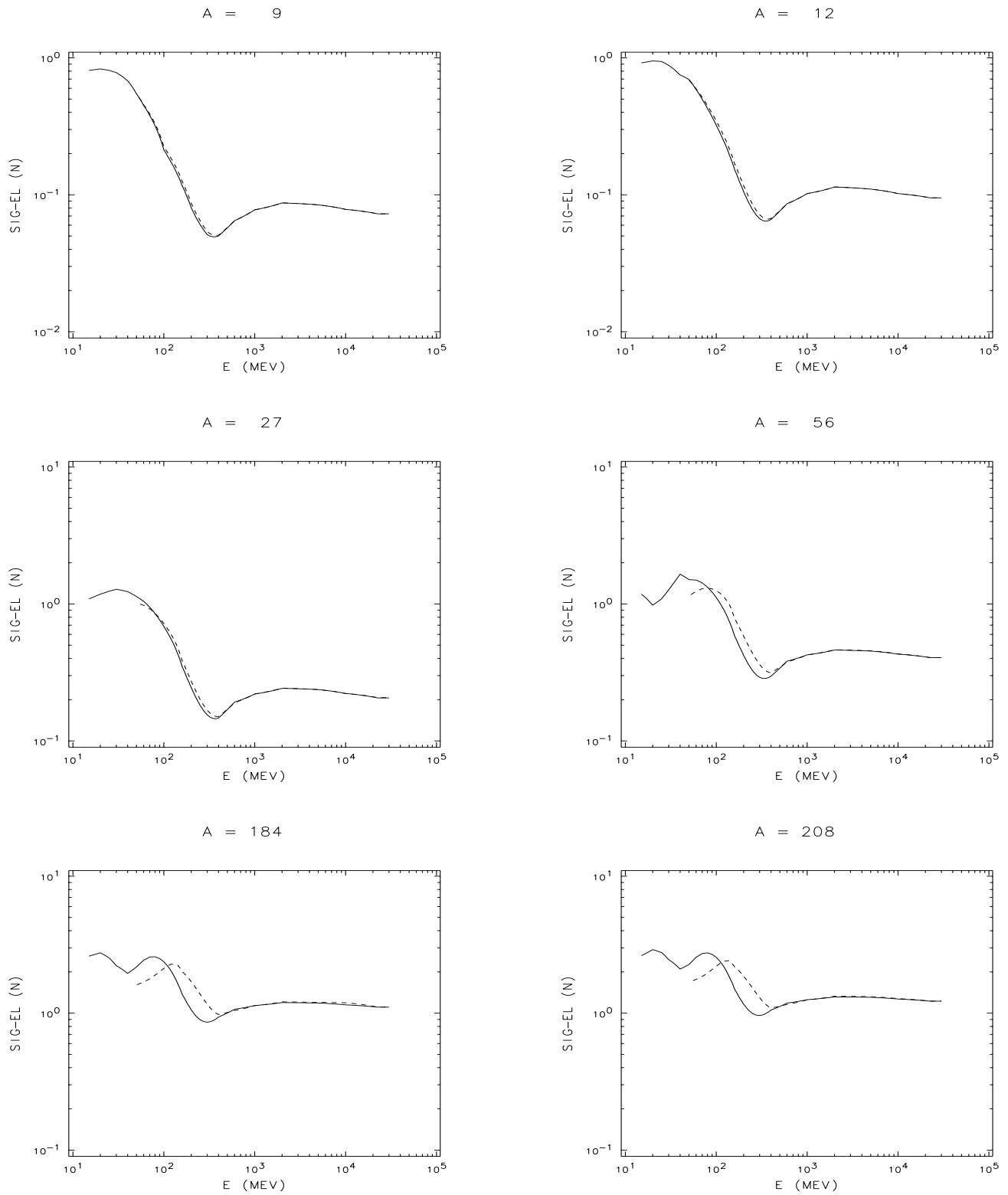


Figure 1: Elastic scattering cross sections for $A = 9, 12, 27, 56, 184,$ and 208 . *Solid line* - neutrons; *dashed line* - protons.

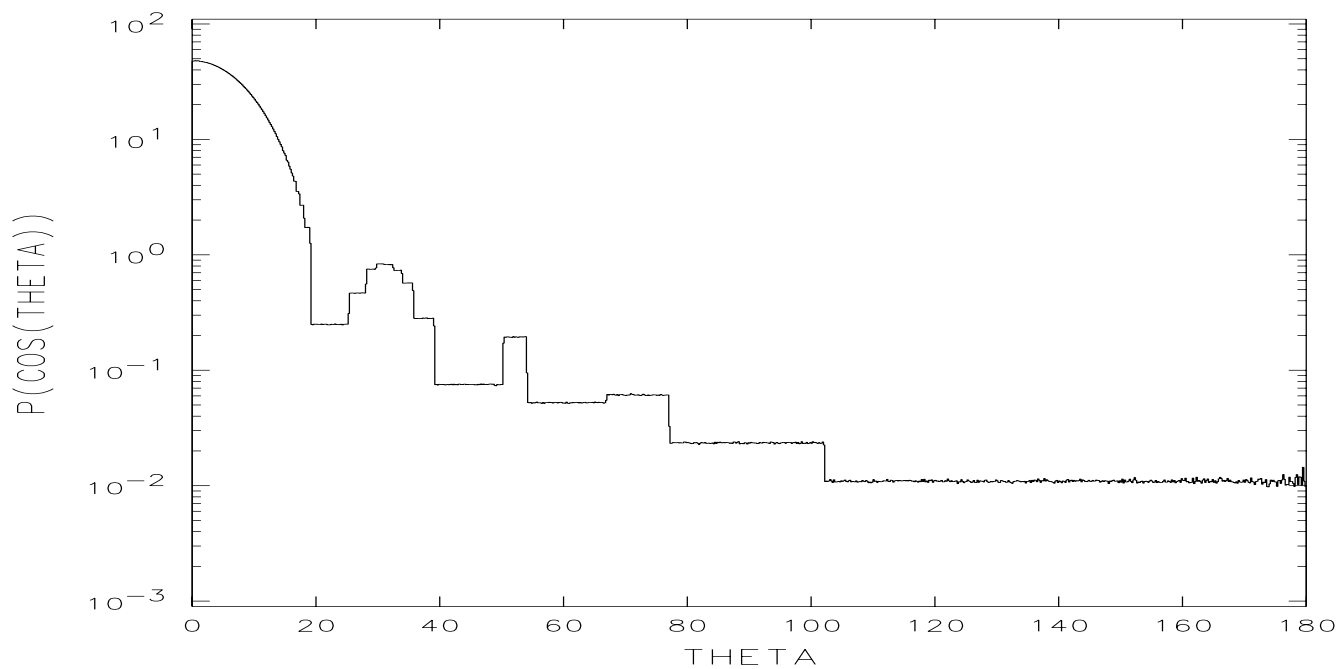


Figure 2: Calculated center of mass angular distribution for 84 MeV neutrons scattered by ^{27}Al obtained from sampling algorithm.

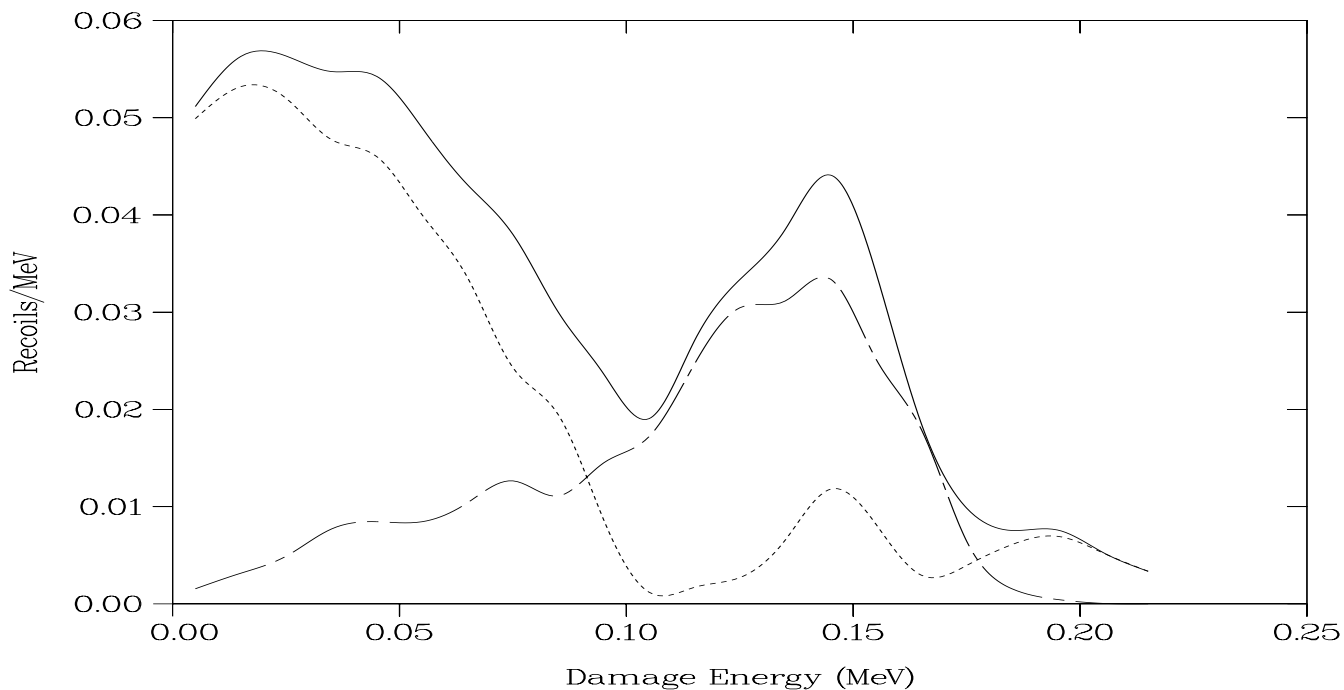


Figure 3: Damage energy spectrum from 100 MeV protons incident on an 0.1 cm ^{27}Al target. The *dashed* line represents the elastic contribution, the *broken* line the nonelastic, and the *solid* line the total. Previously, the total would have been identified with the broken line.

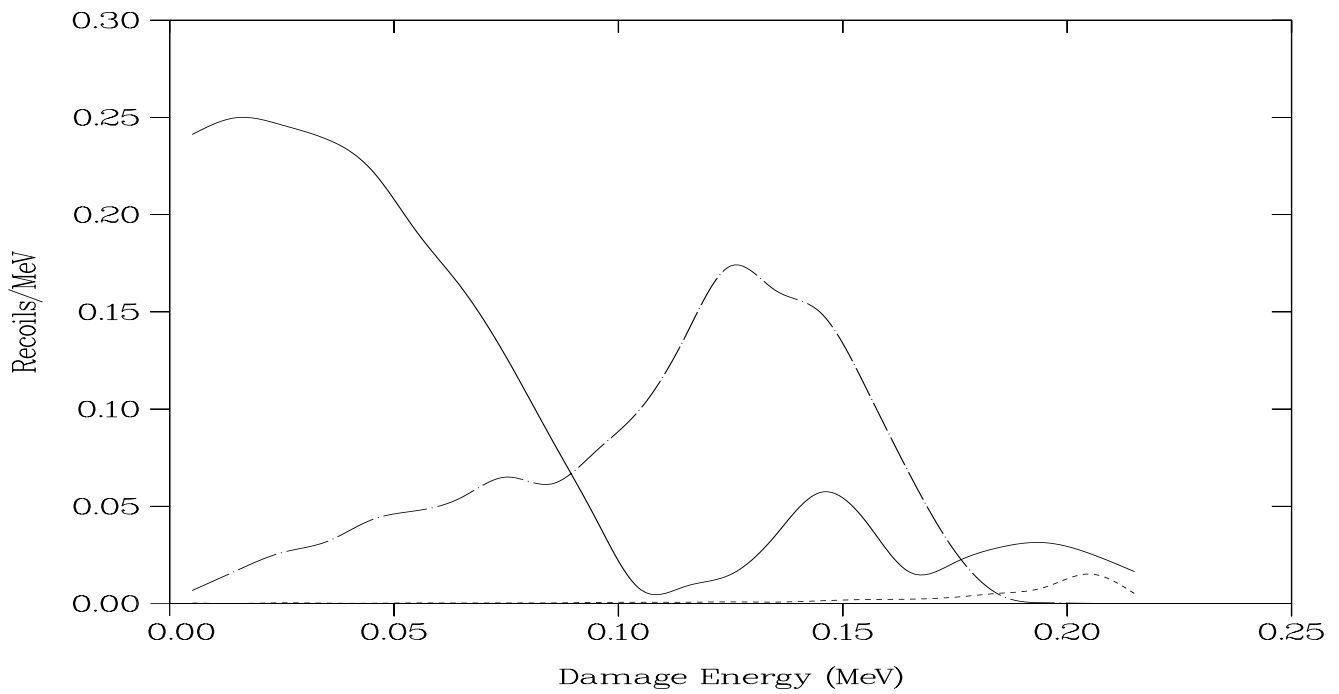


Figure 4: Damage energy spectrum from 100 MeV neutrons incident on an 0.5 cm ^{27}Al target. The *solid* line represents the *new* elastic contribution, the *dashed* line the *old* elastic contribution, and the *broken* line the nonelastic contribution (unchanged).

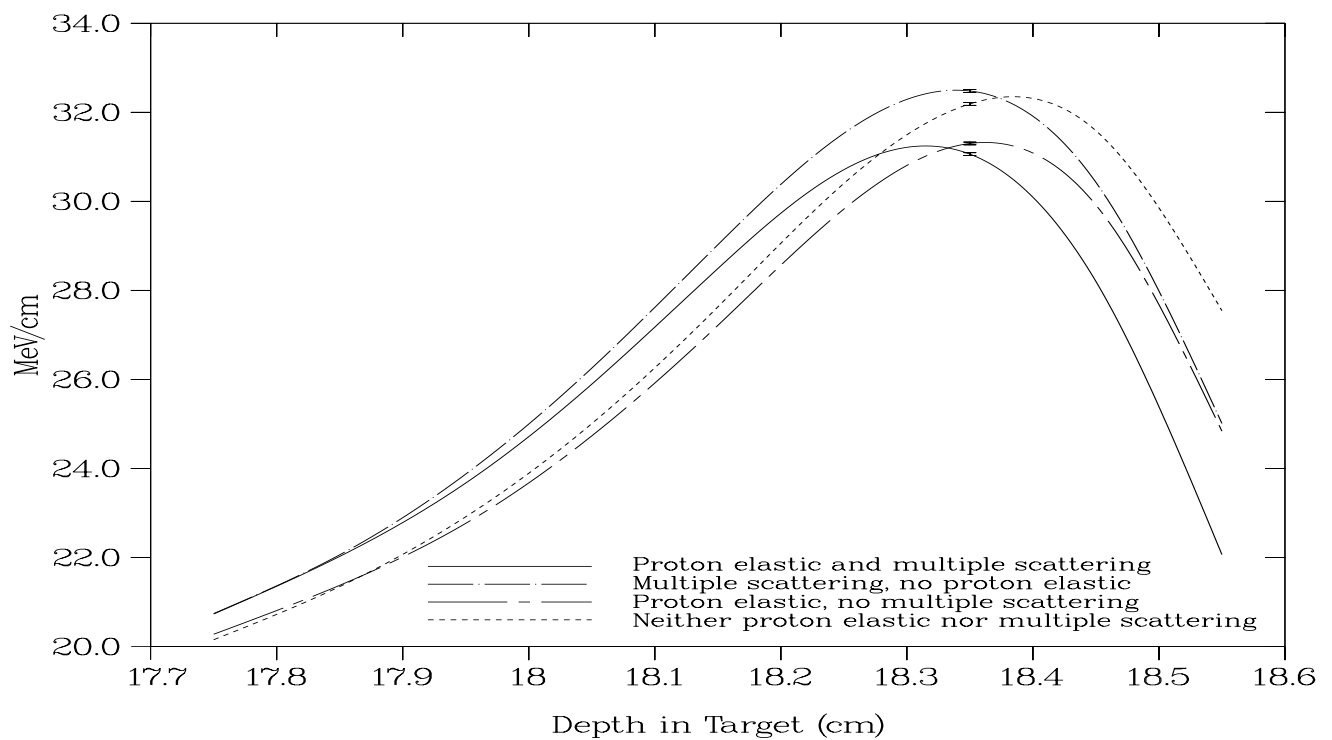


Figure 5: Axial energy deposition from 256 MeV protons incident on a thick ^{27}Al target.